Molecular Catalysis 482 (2020) 110675

Contents lists available at ScienceDirect

Molecular Catalysis

journal homepage: www.elsevier.com/locate/mcat

β-Isocupreidinate–CaAl-layered double hydroxide composites—heterogenized catalysts for asymmetric Michael addition

Gábor Varga[a,b,*], Viktória Kozma[a], Vanessza Judit Kolcsár[a], Ákos Kukovecz[c], Zoltán Kónya[b,c,d], Pál Sipos[b,e], István Pálinkó[a,b,*], György Szőllősi[f]

[a] Department of Organic Chemistry, University of Szeged, Dóm tér 8, Szeged, H-6720, Hungary
[b] Materials and Solution Structure Research Group and Interdisciplinary Excellence Centre, Institute of Chemistry, University of Szeged, Aradi Vértanúk tere 1, Hungary
[c] Department of Applied and Environmental Chemistry, University of Szeged, Rerrich Béla tér 1, Szeged, H-6720, Hungary
[d] MTA-SZTE Reaction Kinetics and Surface Chemistry Research Group, Rerrich Béla tér 1, Szeged, H-6720, Hungary
[e] Department of Inorganic and Analytical Chemistry, University of Szeged, Dóm tér 7, Szeged, H-6720, Hungary
[f] MTA-SZTE Stereochemistry Research Group, University of Szeged, Eötvös utca 6, Szeged, H-6720, Hungary

ARTICLE INFO

Keywords:
CaAl-layered double hydroxide
Intercalation of β-isocupreidiniate
XRD
SEM, IR characterizations
Catalysis of asymmetric Michael addition

ABSTRACT

β-isocupreidinate (β-iCu) anions having well-known structure and catalytic activity in various asymmetric reactions, were incorporated into the interlayer gallery of hydrocalumite (CaAl-LDH) by the partial delamination-restacking method. Silylation of the outer surface of the LDH with trimethyl silane was also employed to avoid the adsorption of β-iCu on the outer surface and to block the basic sites there. The obtained materials were characterized by a range of instrumental methods (X-ray diffractometry, scanning electron microscopy, ATR-IR and grazing incidence IR spectroscopies). The catalytic activities of the composites were tested in the asymmetric Michael addition of β-nitrostyrene and ethyl 2-fluoroacetoacetate. The β-iCu-pillared LDHs proved to be active and recyclable catalysts with very good diastereoselectivities and acceptable and in 2-propanol very good enantioselectivities. The silylated composite retained its activity and diastereoselectivity even in the third repeated run, when heptane was the solvent.

1. Introduction

During the last two decades, in the field of asymmetric synthesis, immense attention has been focused on organocatalysis [1–3]. Due to environmental considerations and pot, atom and step economic reasons, stereoselective organocatalytic reactions gained important role in the efficient and rapid generation of complex molecules [4–9]. Organocatalysts, which have well-known structures, are in many cases easy to synthesize. As compared to well-established transition metal-containing systems, these catalysts allow the stereoselective preparation of chiral building blocks free of metal contaminations, which is of paramount importance in pharmaceutical processes [1–3,5,10]. Accordingly, due to economic, health and social factors, the utilization of optically pure compounds produced by organocatalytic pathways, is dramatically increasing. Chiral organic acids, amines, amino acids, such as L-proline and oligopeptides were found to be efficient catalysts in enantioselective oxidations, reductions, and asymmetric C—C bond formation reactions, such as aldol additions, Mannich, Michael and Diels-Alder reactions [11–18].

Natural cinchona alkaloids and their derivatives are among the most efficient chiral homogeneous organocatalysts [19–22]. Cinchona alkaloids are complex molecules containing five stereocentres. The two rigid units of these molecules, the nucleophilic quinuclidine and the quinoline moieties are connected through a carbinol bridge (see the structure of quinine and quinidine in Fig. 1). The hydroxyl group and substituents on both ring systems allow easy functionalization and fine-tuning of the catalytic properties of these compounds. Accordingly, various cinchona derivatives were found to be highly efficient asymmetric organocatalysts in numerous enantioselective transformations [19–24]. Aromatic hydroxyl groups are useful hydrogen bond donor units in bifunctional organocatalysts [25]. The transformation of the C6′-OMe group in cinchona alkaloids to phenolic hydroxyl leads to cupreine and cupreidine derivatives, which were used as efficient bifunctional catalysts [26,27]. Among these types of cinchona derivatives β-isocupreidine (Fig. 1; the deprotonated version is abbreviated as β-iCu in the followings) is a privileged representative, which besides bearing the phenolic hydroxyl group of acidic character, has a rigid oxazatwistane ring system with low conformational flexibility,

* Corresponding authors at: Department of Organic Chemistry, University of Szeged, Dóm tér 8, Szeged, H-6720, Hungary.
E-mail addresses: gabor.varga5@chem.u-szeged.hu (G. Varga), palinko@chem.u-szeged.hu (I. Pálinkó).

https://doi.org/10.1016/j.mcat.2019.110675
Received 16 September 2019; Received in revised form 9 October 2019; Accepted 16 October 2019
Available online 12 November 2019

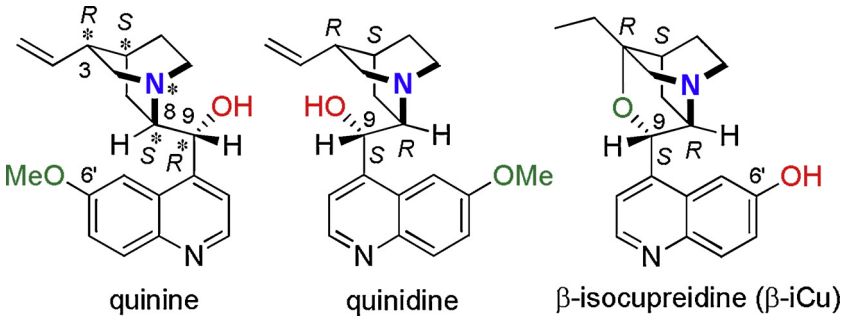

Fig. 1. Structures of the cinchona alkaloids quinine, quinidine and β-isocupreidine.

increased basicity and nucleophilicity. β-iCuH displays appreciable catalytic performance in several asymmetric organocatalytic reactions, such as Morita-Baylis-Hillman reactions, direct aminations, allylic nucleophilic substitutions as well as Michael additions [28–32].

In spite of these attractive features, organocatalysts have been rarely used in industry, which may be related to their insufficient activity under the desired conditions and the difficulties in catalyst separation and recycling [33]. By immobilization of chiral organocatalysts onto/into solid supports, the above-mentioned drawbacks can be diminished or even eliminated. Thus, catalytic materials, which are separable from the reaction mixture, recyclable, adaptable to various reaction conditions and efficient in the continuous production of chiral compounds, may be obtained [34,35]. Despite their advantages, the anchored chiral organocatalysts have gained little attention. This is due to the often-decreased enantioselectivities obtained using such materials, as compared with their homogeneous counterparts. Another reason might be their significantly reduced activity, due to the less accessible active sites of the catalysts and the slow diffusion of the reactants and products to and from these sites determined by the structure and morphology of the support [36]. Deactivation or leaching of the immobilized catalysts from the solid surfaces should also be solved in order to obtain efficient, recyclable materials [36,37].

Accordingly, besides the immobilization methods, utilizing the surface modification of metals, metal oxides as well as resins [38–42], novel procedures have appeared employing mesoporous materials and clays as solid supports for chiral catalysts [43–46]. The latter substances, due to their sterically confined environments, may give the opportunity to increase the enantioselectivity. However, the immobilization of the chiral organocatalysts into the interlayer space of the anionic or cationic clays has been seldom reported, even though various methods have been successfully applied to immobilize organocatalysts between the layers of layered double hydroxides, which showed outstanding activity in various reactions. Among the rare examples, the anionic forms of proline and other amino acids have been incorporated into hydrotalcite or brucite-like layers, and these composites proved to be efficient enantioselective catalysts in enantioselective aldol and asymmetric Michael additions [47–51].

The group of brucite-like materials or layered double hydroxides (LDH) is a family of natural and synthetic substances with a general formula of $[M(II)_{1-x}M(III)_x(OH)_2](Y^{n-})_{x/n} \times yH_2O$, where M(II) and M(III) represent divalent and trivalent metal ions, respectively, and Y^{n-} is the anion situated between the layers [52]. The divalent and trivalent metal cations found in layered double hydroxides belong mainly to the third and fourth periods of the periodic table of elements (divalent cations: Mg^{2+}, Mn^{2+}, Fe^{2+}, Co^{2+}, Ni^{2+}, Cu^{2+}, Zn^{2+}; trivalent cations: Al^{3+}, Mo^{3+}, Fe^{3+}, Co^{3+}, Cr^{3+}, Ga^{3+}) [53]. The ionic radii are mostly in the range of 0.65–0.80 Å for divalent cations and 0.62–0.69 Å for the trivalent ones (there are some exceptions like Al: 0.50 Å and Ba: 1.49 Å). Tetravalent cations such as Zr^{4+} and Sn^{4+} can also be incorporated into the layers. The LDHs consist of hexagonal-shaped brucit-like sheets having positive charge due to partial substitution of M^{2+} with M^{3+}. The uniformly dispersed positive charge is balanced by fully or partially hydrated anions [54–56]. The interlayer anions can be Cl^-, NO_3^-, CO_3^{2-}, *etc.* or various organic anions.

Recently, LDHs were used for the immobilization of β-iCu [32]. However, due to the large dimensions of the cinchona alkaloid derivatives surface-anchored LDH-supported organocatalyst was only obtained. In the present work, β-iCu was incorporated among the layers of the LDH exclusively, and the activity and selectivity of this LDH–β-iCu composites were studied in the Michael addition of ethyl 2-fluoroacetoacetate (**2**) to *trans* β-nitrostyrene (**1**). The partial delamination-restacking method was successfully used to intercalate the organocatalyst exclusively into the interlayer gallery of the LDHs. The as-prepared composites and those recovered following several catalytic cycles were characterized by a range of instrumental techniques.

2. Experimental part

2.1. Materials

All chemicals used in the preparation of the inorganic-organic composites, reagents, solvents of analytical grade applied in the test reaction were purchased from Merck and Sigma-Aldrich and were used as received without further purification. The literature-based preparation of β-iCuH has been described previously [32].

2.2. Syntheses

The CaAl-LDH (hereafter referred to as LDH) was prepared by the co-precipitation method, *via* addition of 3.0 M NaOH solution to a vigorously stirred and N_2-blanketed $CaCl_2 \times 6H_2O/AlCl_3 \times 6H_2O$ solution with 2:1 M ratio at room temperature. The suspension was filtered and dried for 24 h at 60 °C and kept in a desiccator under N_2 until use.

The silylated CaAl-LDH (abbreviated as Sil-LDH) were prepared by a modified co-precipitation method. 6.5 g of $CaCl_2 \times 6H_2O$ and 3.6 g of $AlCl_3 \times 6H_2O$ were dissolved in 100 cm^3 of distilled water (solution A). 5.0 cm^3 trimethylchlorosilane dissolved in 50 cm^3 ethanol was activated by 20% aqueous ammonia solution (solution B). At room temperature, solution B was added dropwise to solution A and the mixture was stirred at pH ~ 13 (set by 3 M NaOH) overnight. The mixture was aged at 80 °C for 12 h. The resulting slurry was filtered, washed with distilled water several times and dried at 60 °C.

The CaAl–β-iCu-LDH (LDH–β-iCu in the followings) and its silylated derivative (Sil-LDH–β-iCu) were produced by the partial delamination method. The previously synthesized chloride-containing (Sil-)LDH (0.5 g) was partially delaminated in an EtOH/DMF 30/70 (vol./vol.) mixture (15 cm^3) by 240-min-long ultrasonic irradiation under inert atmosphere. The reaction mixture was stirred at room temperature for 96 h followed by the addition of 10 cm^3 of 4×10^{-3} M β-iCuH deprotonated with 0.15 M NaOH (aqueous) solution. The slurry was centrifuged (3000 rpm) for 15 min and decanted. A fresh solution of β-isocupreidinate (β-iCu) was added to the solid material again, and the treatment was repeated twice. After the last step, the solid product was filtered, washed with EtOH and dried at 40 °C overnight.

All operations were performed under N_2 blanket to avoid carbonation of the layers and thus the interlayer space by airborne CO_2.

2.3. Characterization techniques

For detection of X-ray diffraction (XRD) patterns, a Rigaku XRD-MiniFlex II instrument utilizing Cu Kα radiation (λ = 0.15418 nm) with 40 kV accelerating voltage at 30 mA was applied. The morphologies of the samples were studied with a scanning electron microscope (SEM, Hitachi S-4700, accelerating voltages of 10–18 kV).

The combination of two different IR techniques was used for detecting the spatial arrangement of the anionic form of β-iCu. The instrument for acquiring the spectra was a BIO-RAD Digilab Division FTS-65A/896 FT-IR spectrophotometer with 4 cm^{-1} resolution. The 4000–600 cm^{-1} wavenumber range was recorded, but the most relevant 1850–600 cm^{-1} range was displayed and discussed. 256 scans were collected for each spectrum. The spectra of each sample were taken using a single reflection diamond ATR accessory and the grazing incidence (GIRA-FTIR) technique (detecting organic material on the surface of the LDH) [56].

2.4. Catalytic test: general procedure

The test reactions were carried out in 4 cm^3 glass vials using magnetic stirring (800 rpm) in a refrigerator set to −20 °C. In a typical experiment, the given amount of catalyst was suspended in 1 cm^3 solvent followed by addition of 0.25 mmol **1**. To the cooled slurry, 0.5 mmol **2** was added, and the reaction was started by turning on the stirrer. Following the given reaction time, the catalyst was centrifuged, the solid material was washed twice with solvent. The unified organic solution was checked for leached out organocatalyst by IR spectroscopy. Following the drying of the organic phase over Na_2SO_4, the products were analysed by gas chromatography. The remaining solid material was dried at room temperature, and reused in successive runs using identical reaction conditions.

Products of the catalytic reactions were identified on the basis of their mass spectra measured on Agilent Techn. 6890 N GC-5973 *inert* MSD system (GC-MSD) equipped with HP-1MS 60 m × 0.25 mm i.d. capillary column [32]. Conversions, diastereomeric ratios and enantioselectivities were calculated based on quantitative analysis carried out using Agilent 7890A GC System equipped with flame ionization detector (FID) and Hydrodex-g-TBDAc 30 m × 0.25 mm (Macherey-Nagel GmbH) chiral capillary column, which allowed the separation of all four ethyl 2-acetyl-2-fluoro-4-nitro-3-phenylbutanoate (**3**) Michael-adduct stereoisomers [30] using decane as internal standard.

Experiments repeated three times showed that the reproducibility of product composition was within ± 1%.

3. Results and discussions

3.1. Silylation and intercalation

In order to find the optimal intercalation conditions of β-iCu into LDH, various synthesis methods were examined. Fig. 2 shows the XRD patterns of the pure chloride-containing LDH (A) and its β-iCu modified derivatives. The XRD patterns of LDHs are usually indexed on the basis of a rhombohedral unit cell, which is analogous to the chloride-containing hydrocalumite. The interlayer distances were calculated on the basis of Bragg's law. Fig. 2B indicates that the intercalation of the cinchona alkaloid was not successful by the reconstruction (dehydration-rehydration) method, because the layered structure was not restored. It is known that molecules, which cannot be intercalated by the reconstruction method, could sometimes be introduced between the layers by applying either the direct anion exchange or the delamination-restacking methods. However, as it is seen in Fig. 2C, the XRD pattern of the LDH modified by anion exchange had the same interlayer

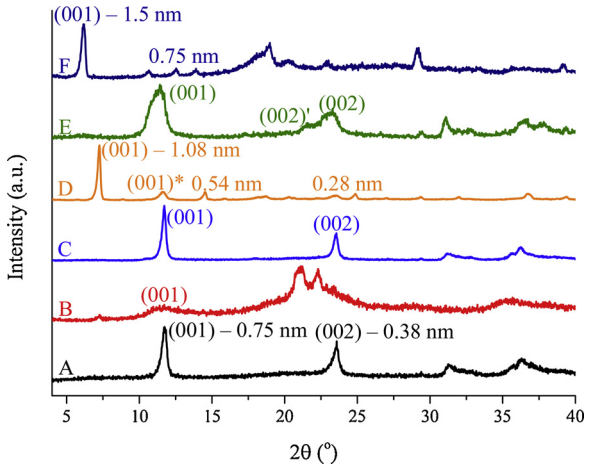

Fig. 2. XRD patterns of A: LDH; B: β-iCu-intercalation (dehydration-rehydration); C: β-iCu-intercalation (direct anion exchange); D: LDH–β-iCu (delamination-restacking); E: Sil-LDH; F: Sil-LDH–β-iCu (delamination-restacking).

distance as the parent LDH. These two composites exhibited interlayer distances close to 0.75 nm. Considering the large dimensions of the β-iCu, the failure in direct intercalation was not surprising.

Accordingly, only the delamination-restacking (Fig. 2D) method seems to give material having the anionic form of the cinchona alkaloid immobilized between the layers (abbreviated as LDH–β-iCu). Based on the XRD pattern of this material, two reaction products are formed following the intercalation process. In the pattern of LDH–β-iCu in Fig. 2D, a series of reflections corresponding to d values of 1.08 (001), 0.54 (002) and 0.27 (003) nm indicated the layered structure with the basal spacing of 1.08 nm. The large interlayer distance confirmed that β-iCu could be introduced into the interlayer region of the restacked LDH. The calculated basal spacing can be ascribed to vertically oriented anions in the interlayer space (the dimensions of β-iCu: 0.782 nm × 0.494 nm × 1.007 nm, the interlayer distance is 1.08 nm – 0.234 nm = 0.846 nm). The interlayer-modified structure exhibited a turbostatic disorder as can be seen from the increased intensity of the 001 reflection compared to the relatively low intensities of the 002 and 003 reflections [57,58]. This effect may occur because of the increase in the 2D character of the material with extensive charge separation and hydration. On the other hand, beside the 1.08 nm-phase, a small amount of the 0.75 nm-phase was also present, which can be interpreted in two ways. Either a single phase is formed in which certain layers contain chloride anions while others contain β-iCu, *i.e.* staging occurred, or two different phases were produced, one of which only contained chloride between the layers, while the other with increased interlayer distance contained β-iCu [59].

Previous studies reported that LDHs behaved as actual catalysts in Michael or nitro Michael reactions due to their basic character, which is ascribed to the Brønsted basic sites, *i.e.* surface OH groups [60,61]. Therefore, in order to examine the catalytic activity of the surface OH groups and the incorporated organocatalyst separately, surface-silylated LDH was also synthesized and intercalated with the anionic form of the cinchona alkaloid. The XRD diffraction pattern of Sil-LDH is displayed in Fig. 2E. In the XRD diffractogram of this material, exactly the same reflections are observed as in that of the parent LDH corresponding to the same d values of 0.75 (001) and 0.38 (002) nm. The broadened peaks indicate decreased crystallinity of the silylated material. Doubled 002 reflections are also observed attributed to the significantly changed hydration of the structure. Starting from the silylated product, a novel intercalated composite was also synthesized. Fig. 2F verifies that the synthesis was successful, furthermore, reflections characteristic to the starting material could not be observed. Its Bragg reflections could also be indexed considering a hexagonal lattice

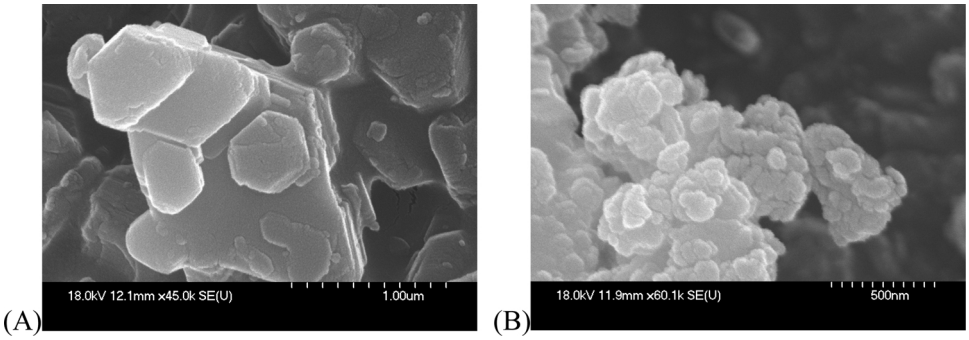

Fig. 3. SEM images of A: LDH–β-iCu; B: Sil-LDH–β-iCu.

with rhombohedral symmetry, similarly to the precursor. The calculated interlayer distance (1.5 nm) increased relative to that of the precursor (0.75 nm), clearly indicating that the intercalation was successful.

In order to provide further evidence for the successful transformation of the parent LDH through intercalation and/or silylation, the as-prepared products were investigated by SEM (Fig. 3). The SEM image of the LDH–β-iCu showed the formation of a material with hexagonally-shaped platelet-like particles (Fig. 3A) confirming the LDH-like structure of the intercalated system [62]. Crystal particles with less regular shapes and smaller particles are observed in the image of Sil-LDH–β-iCu indicating that surface modification influenced the morphology as well as the particles sizes [63].

Since one of the aims of the work is the intercalation of the organocatalyst solely into the interlayer space, determination of the position of the incorporated β-iCu in the LDH–β-iCu was carried out. A comparative IR study was proven to be efficient for determining the local position of the intercalant within the LDH. The ATR-FTIR detection is an available method for observing changes in the bulk as well as on the surface with the predominance of signals originating from the structures of the bulk [64]. As one can see in Fig. 4A, the characteristic vibrations of the interlayer nitrate ions and surface-bound carbonate ions, such as ν_3(interlayer NO_3^-) ~ 1349 cm^{-1}, ν_3(surface CO_3^{2-}) ~ 1415 cm^{-1}, appeared [65]. The vibration bands at 1650 and 785 cm^{-1} were assigned as β(OH) (bending mode) of the water and O–Al–O stretching mode of the LDH structure, respectively [66,66]. On the other hand, since the GIRA-FTIR method has surface-sensitive character [67], significantly altered spectrum is observable in Fig. 4B. The positions of the overlapped and broadened peaks are identical to those of the vibrational modes of the free carbonate ions located at $\nu_{3(surface)}$ ~ 1430 cm^{-1}, $\nu_{2(surface)}$ ~ 890 cm^{-1} and $\nu_{4(surface)}$ ~ 690 cm^{-1} [68]. Therefore, due to the absence of inert atmosphere, the carbon dioxide adsorbed and transformed to carbonate ions on the surface, which can be clearly identified by GIRA-FTIR. As far as the intercalated composite is concerned, beside the above-mentioned absorption bands of carbonate and nitrate ions, new vibrations appeared at 1668 and 1581 cm^{-1} indicating the presence of the anionic form of the cinchona alkaloid (Fig. 4C) [69]. New bands were identified as bending vibration modes of the hydroxyl and amino groups related to β-iCu. The observed significant shifts (1610 → 1668 cm^{-1}) can be ascribed to the interaction of β-iCu with the layer of the LDH host [70,71]. However, based on the GIRA-FTIR measurements, the surface of the composite (Fig. 4D) was similar to that of the parent LDH.

The silylated derivatives of the composites were also studied by both IR techniques (Fig. 5). The characteristic vibrations of the LDH disappeared following silylation, which is consistent with literature results [72,73]. Some of the vibrations related to the trimethyl silane group appeared in all these materials identified as Si—O—M stretching vibrations at ~1000 and 1100 cm^{-1}. The intense peaks at about 1210, 840 and 760 cm^{-1} can be assigned to the bending, rocking and stretching vibrations of Si–Me, respectively, corresponding to $–Si(Me)_x–$ units from trimethyl silane [74]. The broadened peaks at about 1350 and 1450 cm^{-1} were assigned as nitrate and carbonate ions distorted during the silylation process, which highly influenced the hydration state of the LDH [75,76]. After intercalation, the above-assigned vibrations such as hydroxyl vibrations appeared indicating the successful inclusion of the anionic form of the cinchona alkaloid. GIRA-FTIR spectrum of the intercalated system resembled the spectrum of the non-intercalated composite.

On the basis of IR measurements, it can be stated that β-iCu is overwhelmingly resides among the layers of the LDH in both composites.

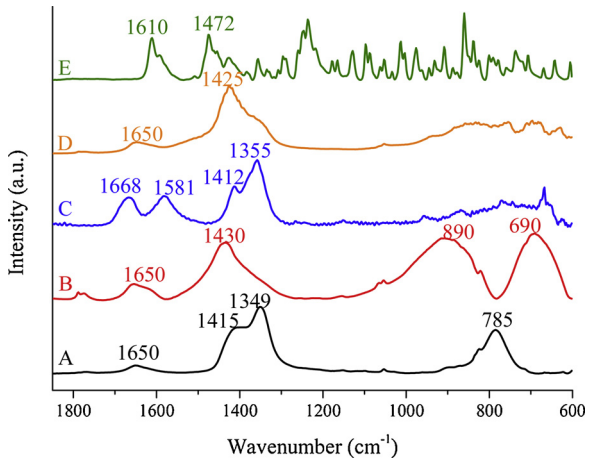

Fig. 4. IR spectra of A: LDH (ATR-FTIR); B: LDH (GIRA-FTIR); C: LDH–β-iCu (ATR-FTIR); D: LDH–β-iCu (GIRA-FTIR); E: Na-β-iCu (ATR-FTIR).

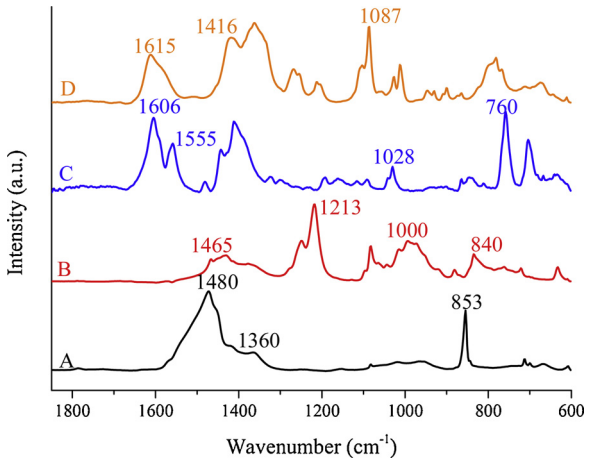

Fig. 5. IR spectra of: A: Sil-LDH (ATR-FTIR); B: Sil-LDH (GIRA-FTIR); C: Sil-LDH–β-iCu (ATR-FTIR); D: Sil-LDH–β-iCu (GIRA-FTIR).

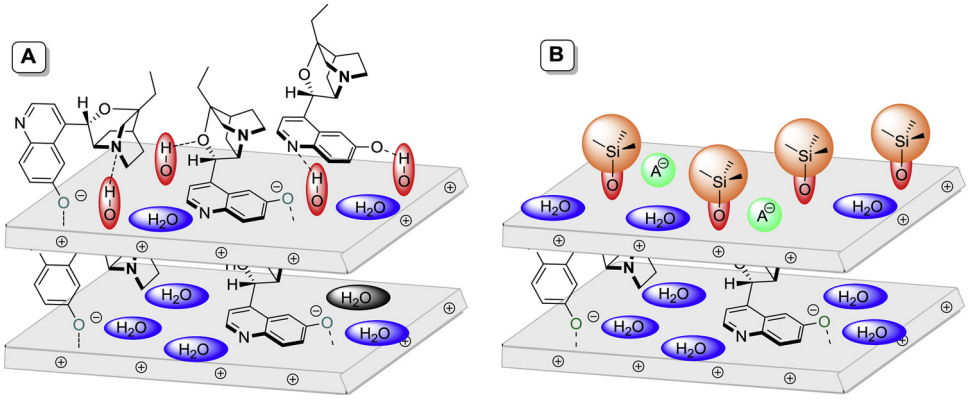

Fig. 6. Possible structures for LDH–β-iCu (A) and Sil-LDH–β-iCu based on XRD and ATR- and GIRA-FTIR measurements.

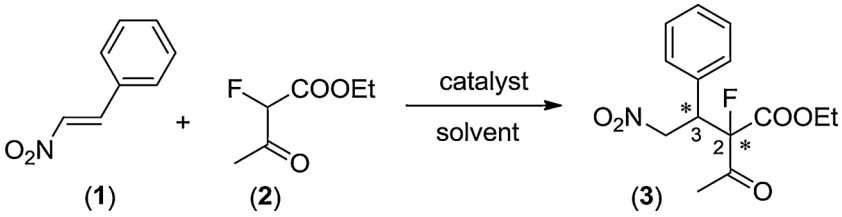

Scheme 1. The Michael addition of ethyl 2-fluoroacetoacetate (**2**) to *trans* β-nitrostyrene (**1**).

Table 1
Results of the Michael addition catalysed by the unmodified CaAl-LDH, β-iCu as homogeneous catalyst and β-iCu intercalated in non-silylated and silylated CaAl-LDH[a].

Entry	catalyst	solvent	conv (%)[b]	dr[b]	ee (%)[c]
1	–	DCE	< 1	–	–
2	β-iCu	DCE	99	85/15	98; 96
3	CaAl-LDH	heptane	72	–	–
4	LDH–β-iCu	DCE	89	83/17	29; 26
5	LDH–β-iCu	toluene	94	73/27	22; 26
6	LDH–β-iCu	heptane	90	65/35	3; 4
7	LDH–β-iCu	2-propanol	> 99	75/25	95; 82
8	Sil-LDH–β-iCu	DCE	> 99	80/20	28; 24
9	Sil-LDH–β-iCu	toluene	> 99	73/27	22; 28
10	Sil-LDH–β-iCu	heptane	> 99	67/33	19; 11
11	Sil-LDH–β-iCu	2-propanol	> 99	78/22	97; 94

[a] Reaction conditions: catalyst 20 mg, 0.25 mmol of **1**, 0.5 mmol of **2**, 1 cm^3 solvents, −20 °C, 22 h.
[b] Conversions (conv) and diastereomeric ratios (dr) determined by GC-FID.
[c] Enantiomeric excesses (ee), the configuration of the excess enantiomers were assigned based on previous studies and GC-FID analysis as 2*R*,3*R* and 2*S*,3*R* [32].

Possible structures for the non-silylated and silylated intercalated LDHs, mainly for helping visualisation, are given in Fig. 6A and B, respectively.

3.2. Catalytic behaviour of the materials

The composite materials obtained, LDH–β-iCu and Sil-LDH–β-iCu, were tested as catalysts in the Michael addition of **2** to **1** (Scheme 1). Results obtained in various solvents are summarized in Table 1.

The obtained diastereomeric ratios and enantiomeric excess values confirmed that these composites catalysed the Michael addition, and the catalysts were the chiral solid hybrid materials. The material prepared by the inclusion of the anionic form of the cinchona alkaloid in the parent LDH provided lower conversions in every solvent tested than those obtained using the silylated composite. A possible explanation of this activity difference may be the decreased hydrophilicity of the interlamellar space following silylation, which favours the migration of

Table 2
Results of the Michael addition over the reused β-iCu intercalated in non-silylated and silylated CaAl-LDH[a].

catalyst	nr. of reuse	solvent	conv (%)[b]	dr[b]	ee (%)[c]
LDH–β-iCu	1	2-propanol	83	66/34	88; 77
	2	2-propanol	< 4	53/47	10; 12
Sil-LDH–β-iCu	1	DCE	43	78/22	19; 18
Sil-LDH–β-iCu	1	toluene	> 99	74/26	16; 21
	2	toluene	65	73/27	10; 12
Sil-LDH–β-iCu	1	heptane	> 99	67/33	10; 6
	2	heptane	> 99	66/34	7; 4
	3	heptane	98	66/34	4; 2

[a] Reaction conditions: catalyst 20 mg, 0.25 mmol of **1**, 0.5 mmol of **2**, 1 cm^3 solvents, −20 °C, 22 h.
[b] Conversions (conv) and diastereomeric ratios (dr) determined by GC-FID.
[c] Enantiomeric excesses (ee), the configuration of the excess enantiomers were assigned based on previous studies and GC-FID analysis as 2*R*,3*R* and 2*S*,3*R* [32].

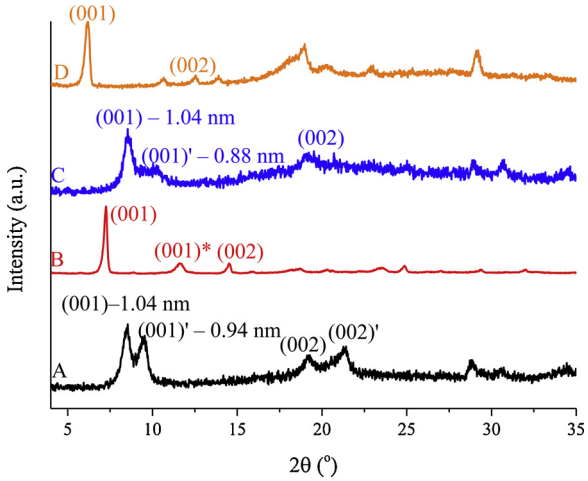

Fig. 7. XRD patterns of A: used (in toluene, 2 times) and B: as-prepared LDH–β-iCu; C: used (in heptane, 4 times) and D: as-prepared Sil-LDH–β-iCu.

the reactants and the products to/from the chiral active sites. It is known that cinchona alkaloids have rich conformational behaviour, due to rotations around the C^8–C^9 and C^9–C4′ axes [20–23,77]. Although in the isocinchona alkaloids the former is hindered, rotation around the C^9–C4′ bond still allows the formation of some conformers [78]. However, the similar (quite high) diastereomeric ratios (dr) and (the moderate) enantiomeric excess (ee) values obtained with both the LDH–β-iCu and Sil-LDH–β-iCu (except in heptane) indicated similar arrangement of the immobilized β-isocupreidinate.

The dr and ee values were calculated the following way:

$$dr = [c(S,S) - c(R,R)]/[c(R,S) - c(S,R)],$$

$$ee = 100 \times [c(S,S) - c(R,R)/[c(S,S) + c(R,R)] \text{ and } 100 \times [c(R,S) - c(S,R)]/[c(R,S) + c(S,R)]$$

where c(S,S), c(R,R), c(R,S) and c(S,R) are the concentrations of the Michael adducts, and there were no other products.

The low ee values obtained with LDH–β-iCu in heptane could be due to the difficult approach of the reactants to the chiral sites found in a hydrophilic environment, thus the surface basic centres of the inorganic material only catalysed the reaction. Upon reuse, the activity as well as the ee values decreased (Table 2). It is to be noted that Sil-LDH–β-iCu could keep its activity in four uses in heptane, and the diastereomer ratio did not decrease either. These results are quite probably originated in the largely hydrophobic environment due to the solvent as well as the silylated composite. The ee value decreased during the repeated runs even on this catalyst.

The enantioselectivites were found to be quite good in 2-propanol. We think that this solvent partially replaced the interlayer water molecules, and created an environment in which the accessibility of the chiral centres of the alkaloid modifier was increased. The other solvents either could not replace the interlayer water molecules or even if they partially could, the new environment was not advantageous for exposing the chiral centres to the incoming reactants.

The catalysts were recovered from the reaction mixtures by centrifuging the slurries and washing the solids before their X-ray diffractograms were registered. Substances with high crystallinities were obtained (Fig. 7). The (001) reflections of these materials (Fig. 7A and C) indicate that the recovered substances kept their layered structure. The basal distance of the major phase was 1.04 nm and that of the minor phase was ~0.90 nm. Even this latter value was larger than that found for the parent LDH (0.75 nm). The major phase contained β-iCu immobilized between the layers. Change in the hydration degree of the interlayer gallery and/or the rearrangement of the interlayer region due to the conformational transition of the alkaloid may explain the lower interlamellar distance. Leaching of the organocatalyst was not observed either from the silylated or the non-silylated composites.

4. Conclusions

It was shown that the inclusion of these bulky anionic cinchona alkaloids into the interlamellar space was possible by the delamination-restacking method. Furthermore, the silylated derivatives of these composites have also been synthesized. The composites were characterised by several methods (XRD, two IR techniques, SEM), and it was proven that the organocatalyst was between the layers, indeed. Materials containing immobilized β-iCu were tested as catalysts in the asymmetric Michael addition of a C-nucleophile to β-nitrostyrene. In general, the diastereoselectivities were high, the enantioselectivities were acceptable in most cases and very good using 2-propanol as solvent. There was no leaching of β-iCu during the reactions; however, rearrangement of intercalated organocatalyst may have occurred during the reactions explaining the decreasing enantioselectivity in the repeated runs.

Declaration of Competing Interest

None.

Acknowledgements

This work was supported by the Hungarian Government and the European Union through grant GINOP-2.3.2-15-2016-00013. G. Varga thanks for the postdoctoral fellowship under the grant PD 128189.

References

[1] A. Berkessel, H. Groger, Asymmetric Organocatalysis: From Biomimetic Concepts to Applications in Asymmetric Synthesis, Wiley-VCH, Weinheim, 2005.
[2] B. List, K. Maruoka, Science of Synthesis: Asymmetric Organocatalysis, Thieme, Stuttgart, 2012.
[3] P.I. Dalko, Comprehensive Enantioselective Organocatalysis: Catalysts, Reactions and Applications Vols. 1–3 Wiley-VCH, Weinheim, 2013.
[4] G.L. Hua, C. Li, X.F. Wang, L.Q. Lu, J.R. Chen, W.J. Xiao, Enantioselective synthesis of chromans with a quaternary stereogenic centre through catalytic asymmetric cascade reactions, ACS Catal. 1 (2011) 221–226.
[5] T. Shi, Z. Guo, H. Yu, J. Xie, Y. Zhong, W. Zhu, Atom-economic synthesis of optically active Warfarin anticoagulant over a chiral MOF organocatalyst, Adv. Synth. Catal. 355 (2013) 2538–2543.
[6] R. Bharti, R. Parvin, One-pot synthesis of highly functionalized tetrahydropyridines: a camphor sulfonic acid catalysed multicomponent reaction, J. Heterocyclic Chem. 52 (2015) 1806–1811.
[7] V.J. Lillo, J.M. Saá, Towards enzyme-like, sustainable catalysis: switchable, highly efficient asymmetric synthesis of enantiopure Biginelli dihydropyrimidinones or hexahydropyrimidinones, Chem. Eur. J. 22 (2016) 17182–17186.
[8] H. Wei, M. Bao, K. Dong, L. Qiu, B. Wu, W. Hu, X. Xu, Enantioselective oxidative cyclization/Mannich addition enabled by gold (I)/chiral phosphoric acid cooperative catalysis, Angew. Chem. Int. Ed. 57 (2018) 17200–17204.
[9] Gy. Szőllősi, Asymmetric one-pot reactions using heterogeneous chemical catalysis: recent steps towards sustainable processes, Catal. Sci. Technol. 8 (2018) 389–422.
[10] F. Xu, M. Zacuto, N. Yoshikawa, R. Desmond, S. Hoerrner, T. Itoh, M. Journet, G.R. Humphrey, C. Cowden, N. Strotman, P. Devine, Asymmetric synthesis of telcagepant, a CGRP receptor antagonist for the treatment of migraine, J. Org. Chem. 75 (2010) (2010) 7829–7841.
[11] W. Notz, F. Tanaka, C.F. Barbas, Enamine-based organocatalysis with proline and diamines: the development of direct catalytic asymmetric aldol, Mannich, Michael, and Diels – Alder reactions, Acc. Chem. Res. 37 (2004) 580–591.
[12] X. Yu, W. Wang, Organocatalysis: asymmetric cascade reactions catalysed by chiral secondary amines, Org. Biomol. Chem. 6 (2008) 2037–2046.
[13] R. Mahrwald, Enantioselective Organocatalyzed Reactions I, Enantioselective Oxidation, Reduction, Functionalization and Desymmetrization, Springer, Dordrecht, 2011.
[14] R. Mahrwald, R, Enantioselective Organocatalyzed Reactions II, Asymmetric C–C Bond Formation Processes, Springer, Dordrecht, 2011.
[15] M. Tsakos, C.G. Kokotos, Primary and secondary amine-(thio)ureas and squaramides and their applications in asymmetric organocatalysis, Tetrahedron 69 (2013) 10199–10222.
[16] Y.L. Sun, L. Wei, M. Shi, Applications of chiral thiourea-amine/phosphine organocatalysts in catalytic asymmetric reactions, ChemCatChem 9 (2017) 718–727.
[17] S. Nießing, C. Janiak, Studies on catalytic activity of MIL-53 (Al) and structure analogue DUT-5 (Al) using bdc-and bpdc-ligands functionalized with L-proline in a solid-solution mixed-linker approach, Mol. Catal. 467 (2019) 70–77.
[18] J. Xu, J. Pang, D. Feng, X. Ma, Jorgensen–hayashi organocatalyst/Brønsted acid-tethered multifunctional polymeric nanospheres for complex asymmetric multicomponent/multicatalysed organocatalysis: heterogeneous Michael/Michael/aldol organocascade and [4 + 2] cycloaddition reactions, Mol. Catal. 443 (2017) 139–147.
[19] K. Kacprzak, J. Gawroński, Cinchona alkaloids and their derivatives: versatile catalysts and ligands in asymmetric synthesis, Synthesis (2001) 961–998.
[20] C.E. Song, Cinchona Alkaloids in Synthesis and Catalysis, Ligands, Immobilization and Organocatalysis, Wiley-VCH, Weinheim, 2009.
[21] T. Marcelli, H. Hiemstra, Cinchona alkaloids in asymmetric organocatalysis, Synthesis (2010) 1229–1279.
[22] M.S. Ullah, S. Itsuno, Synthesis of cinchona alkaloid squaramide polymers as bifunctional chiral organocatalysts for the enantioselective Michael addition of β-ketoesters to nitroolefins, Mol. Catal. 438 (2017) 239–244.
[23] E.M.O. Yeboah, S.O. Yeboah, G.S. Singh, Recent applications of cinchona alkaloids and their derivatives as catalysts in metal-free asymmetric synthesis, Tetrahedron 67 (2011) 1725–1762.
[24] P.J. Boratyński, Dimeric cinchona alkaloids, Mol. Divers. 19 (2015) 385–422.
[25] P. Chauhan, S.S. Chimni, Aromatic hydroxyl group – a hydrogen bonding activator in bifunctional asymmetric organocatalysis, RSC Adv. 2 (2012) 737–758.
[26] T. Marcelli T, J.H. van Maarseveen, H. Hiemstra, Cupreines and cupreidines: an emerging class of bifunctional cinchona organocatalysts, Angew. Chem. Int. Ed. 45 (2006) 7496–7504.
[27] L.A. Bryant, R. Fanelli, A.J.A. Cobb, Cupreines and cupreidines: an established class of bifunctional cinchona organocatalysts, Beilstein J. Org. Chem. 12 (2016)

429–443.
[28] Y. Iwabuchi, M. Nakatani, N. Yokoyama, S.J. Hatakeyama, S.J, Chiral amine-catalysed asymmetric Baylis-Hillman reaction: a reliable route to highly enantiomerically enriched (α-methylene-β-hydroxy) esters, J. Am. Chem. Soc. 121 (1999) 10219–10220.
[29] M. Shi, Y.M. Xu, Catalytic Y.M, Asymmetric Baylis-Hillman reaction of imines with methyl vinyl ketone and methyl acrylate, Angew. Chem. Int. Ed. 41 (2002) 4507–4510.
[30] S. Saaby, M. Bella, K.A. Jørgensen, Asymmetric construction of quaternary stereocenters by direct organocatalytic amination of α-substituted α-cyanoacetates and β-dicarbonyl compounds, J. Am. Chem. Soc. 126 (2004) 8120–8121.
[31] Y. Du, X. Han, X. Lu, Alkaloids-catalysed regio- and enantioselective allylic nucleophilic substitution of tert-butyl carbonate of the Morita-Baylis-Hillman products, Tetrahedron Lett. 45 (2004) 4967–4971.
[32] Gy. Szőllősi, L. Kovács, V. Kozma, V.J. Kolcsár, Asymmetric Michael addition catalysed by a cinchona alkaloid derivative non-covalently immobilized on layered inorganic supports, Reac. Kinet. Mech. Cat. 121 (2017) 293–306.
[33] R.T. Baker, S. Kobayashi, W. Leitner, Divide et impera – multiphase, green solvent and immobilization strategies for molecular catalysis, Adv. Synth. Catal. 348 (2006) 1337–1340.
[34] I.M. Mándity, S.B. Ötvös, Gy. Szőllősi, F. Fülöp, Harnessing the versatility of continuous-flow processes: Selective and efficient reactions, Chem. Rec. 16 (2016) 1018–1033.
[35] G. Xie, D. Feng, X. Ma, 9-Amino (9-deoxy) epi-cinchona alkaloid-tethered aluminium phosphonate architectures for heterogeneous cooperative catalysis: asymmetric aldol and double-Michael cascade reaction, Mol. Catal. 434 (2017) 86–95.
[36] C. Li, Chiral synthesis on catalysts immobilized in microporous and mesoporous materials, Catal. Rev. 46 (2004) 419–492.
[37] C. Yu, J. He, Synergic catalytic effects in confined spaces, Chem. Commun. 48 (2012) 4933–4940.
[38] A.V. Malkov, M. Figlus, G. Cooke, S.T. Caldwell, G. Rabani, M.R. Prestly, P. Kočovský, Organocatalysts immobilised onto gold nanoparticles: application in the asymmetric reduction of imines with trichlorosilane, Org. Biomol. Chem. 7 (2009) 1878–1883.
[39] L. Zhong, J. Xiao, C. Li, An unexpected inversion of enantioselectivity in direct asymmetric aldol reactions on a unique L-proline/γ-Al_2O_3 catalyst, J. Catal. 243 (2006) 422–445.
[40] F.G. Finelli, L.S. Miranda, R.O. de Souza, Expanding the toolbox of asymmetric organocatalysis by continuous-flow process, Chem. Commun. 51 (2015) 3708–3722.
[41] J. Lu, P.H. Toy, Organic polymer supports for synthesis and for reagent and catalyst immobilization, Chem. Rev. 109 (2009) 815–838.
[42] J.D. Revell, D. Gantenbein, P. Krattinger, H. Wennemers, Solid-supported and pegylated H–Pro–Pro–Asp–NHR as catalysts for asymmetric aldol reactions, Biopolymers 84 (2006) 105–113.
[43] A. Stein, B.J. Melde, R.C. Schroden, Hybrid inorganic-organic mesoporous silicates – nanoscopic reactors coming of age, Adv. Mater. 12 (2000) 1403–1419.
[44] A. Zamboulis, N. Moitra, J.J. Moreau, X. Cattoen, M.W.C. Man, Hybrid materials: versatile matrices for supporting homogeneous catalysts, J. Mater. Chem. 20 (2010) 9322–9338.
[45] V. Srivastava, K. Gaubert, M. Pucheault, M. Vaultier, Organic-inorganic hybrid materials for enantioselective organocatalysis, ChemCatChem 1 (2009) 94–98.
[46] Gy. Szőllősi, D. Gombkötő, A.Zs. Mogyorós, F. Fülöp, Surface-improved asymmetric Michael addition catalysed by amino acids adsorbed on Laponite, Adv. Synth. Catal. 360 (2018) 1992–2004.
[47] S. Vijaikumar, A. Dhakshinamoorthy, K. Pitchumani, l-Proline anchored hydrotalcite clays: an efficient catalyst for asymmetric Michael addition, Appl. Catal. A Gen. 340 (2008) 25–32.
[48] Z. An, W. Zhang, H. Shi, J. He, An effective heterogeneous L-proline catalyst for the asymmetric aldol reaction using anionic clays as intercalated support, J. Catal. 241 (2006) 319–327.
[49] M. Sipiczki, D.F. Srankó, Gy. Szőllősi, Á. Kukovecz, Z. Kónya, P. Sipos, I. Pálinkó, Preparation, characterisation and some reactions of organocatalysts immobilised between the layers of a CaFe-layered double hydroxide, Top. Catal. 55 (2012) 858–864.
[50] L.W. Zhao, Shi H.M, J.Z. Wang, J. He, Nanosheet-enhanced asymmetric induction of chiral α-amino acids in catalytic aldol reaction, Chem. Eur. J. 18 (2012) 15323–15329.
[51] L. Zhang, S. Luo, J.P. Cheng, Non-covalent immobilization of asymmetric organocatalysts, Catal. Sci. Technol. 1 (2011) 507–516.
[52] D.G. Evans, R.C.T. Slade, Structural aspects of layered double hydroxides, Struct. Bond. 119 (2006) 1–87.
[53] G.R. Williams, D. O'Hare, Towards understanding, control and application of layered double hydroxide chemistry, J. Mater. Chem. 16 (2006) 3065–3074.
[54] G. Varga, Á. Kukovecz, Z. Kónya, L. Korecz, Sz. Muráth, Z. Csendes, G. Peintler, S. Carlson, P. Sipos, I. Pálinkó, Mn (II)–amino acid complexes intercalated in CaAl-layered double hydroxide – well-characterized, highly efficient, recyclable oxidation catalysts, J. Catal. 335 (2016) 125–134.
[55] F. Zhang, L. Zhao, H. Chen, S. Xu, D.G. Evans, X. Duan, Corrosion resistance of superhydrophobic layered double hydroxide films on aluminum, Angew. Chem. Int. Ed. 47 (2008) 2466–2469.
[56] Y. Zhao, F. Li, R. Zhang, D.G. Evans, X. Duan, Preparation of layered double-hydroxide nanomaterials with a uniform crystallite size using a new method involving separate nucleation and aging steps, Chem. Mater. 14 (2002) 4286–4291.
[57] X.Y. Jin, K.J. Kim, H.S. Lee, Grazing incidence reflection absorption Fourier transform infrared (GIRA-FTIR) spectroscopic studies on the ferroelectric behavior of poly (vinylidene fluoride–trifluoroethylene) ultrathin films, Polymer 46 (2005) 12410–12415.
[58] B.R. Venugopal, C. Shivakumara, M. Rajamathi, Effect of various factors influencing the delamination behavior of surfactant intercalated layered double hydroxides, J. Colloid Interface Sci. 294 (2006) 234–239.
[59] N. Iyi, K. Fujii, K. Okamoto, T. Sasaki, Factors influencing the hydration of layered double hydroxides (LDHs) and the appearance of an intermediate second staging phase, Appl. Clay Sci. 35 (2007) 218–227.
[60] D. Tichit, B. Coq, Catalysis by hydrotalcites and related materials, Cattech 7 (2003) 206–217.
[61] M. Mokhtar, T.S. Saleh, S.N. Basahel, Mg-Al hydrotalcites as efficient catalysts for aza-Michael addition reaction: a green protocol, J. Mol. Catal. A 353 (2012) 122–131.
[62] Z.P. Xu, P.S. Braterman, High affinity of dodecylbenzene sulfonate for layered double hydroxide and resulting morphological changes, J. Mater. Chem. 13 (2003) 268–273.
[63] Q. Tao, J. Yuan, R.L. Frost, H. He, P. Yuan, J. Zhu, Effect of surfactant concentration on the stacking modes of organo-silylated layered double hydroxides, Appl. Clay Sci. 45 (2009) 262–269.
[64] N. Nagai, H. Hashimoto, FT-IR-ATR study of depth profile of SiO_2 ultrathin films, Appl. Surf. Sci. 172 (2001) 307–311.
[65] J.T. Kloprogge, D. Wharton, L. Hickey, R.L. Frost, Infrared and Raman study of interlayer anions CO_3^{2-}, NO_3^-, SO_4^{2-} and ClO_4^- in Mg/Al-hydrotalcite, Am. Miner. 87 (2002) 623–629.
[66] V. Rives, S. Kannan, Layered double hydroxides with the hydrotalcite-type structure containing Cu^{2+}, Ni^{2+} and Al^{3+}, J. Mater. Chem. 10 (2000) 489–495.
[67] L.J. Fina, Depth profiling of polymer surfaces with FT-IR spectroscopy, Appl. Spectrosc. Rev. 29 (1994) 309–365.
[68] H. Xu, Dielectric properties and ferroelectric behavior of poly(vinylidene fluoride-trifluoroethylene) 50/50 copolymer ultrathin films, J. Appl. Polym. Sci. Symp. 80 (2001) 2259–2266.
[69] Y. Suetsugu, I. Shimoya, J. Tanaka, Configuration of carbonate ions in apatite structure determined by polarized infrared spectroscopy, J. Am. Ceram. Soc. 81 (1998) 746–748.
[70] A. Nakano, M. Ushiyama, Y. Iwabuchi, S. Hatakeyama, Synthesis of an enantiocomplementary catalyst of β-isocupreidine (β-ICD) from quinine, Adv. Synth. Catal. 347 (2005) 1790–1796.
[71] M.J. Hernandez-Moreno, M.A. Ulibarri, J.L. Rendon, C.J. Serna, IR characteristics of hydrotalcite-like compounds, Phys. Chem. Miner. 12 (1985) 34–38.
[72] V.R. Constantino, T.J. Pinnavaia, T.J, Basic properties of $Mg^{2+}_{1-x}Al^{3+}_x$ layered double hydroxides intercalated by carbonate, hydroxide, chloride, and sulfate anions, Inorg. Chem. 34 (1995) 883–892.
[73] Q. Tao, H. He, R.L. Frost, P. Yuan, J. Zhu, Nanomaterials based upon silylated layered double hydroxides, Appl. Surf. Sci. 255 (2009) 4334–4340.
[74] Y. Xu, D. Su, H. Feng, X. Yan, N. Liu, Y. Sun, Continuous sol-gel derived SiOC/HfO_2 fibers with high strength, RSC Adv. 5 (2015) 35026–35032.
[75] G.M. Renlund, S. Prochazka, R.H. Doremus, Silicon oxycarbide glasses: part II. Structure and properties, J. Mater. Res. 6 (1991) 2716–2734.
[76] N. Iyi, T. Matsumoto, Y. Kaneko, K. Kitamura, Deintercalation of carbonate ions from a hydrotalcite-like compound: enhanced decarbonation using acid–salt mixed solution, Chem. Mater. 16 (2004) 2926–2932.
[77] A. Urakawa, D.M. Meier, H. Rüegger, A. Baiker, Conformational behavior of cinchonidine revisited: a combined theoretical and experimental study, J. Phys. Chem. A 112 (2008) 7250–7255.
[78] S. Kristyán, Origin of proposed mechanistic models in heterogeneous catalytic enantioselective hydrogenation of pyruvates comes from the conformation properties of internal rotation of cinchona alkaloids, J. Phys. Chem. C 113 (2009) 21700–21712.